Optics Communications 380 (2016) 357–360

Contents lists available at ScienceDirect

Optics Communications

journal homepage: www.elsevier.com/locate/optcom

Power scaling of blue-diode-pumped Pr:YLF lasers at 523.0, 604.1, 606.9, 639.4, 697.8 and 720.9 nm

Saiyu Luo, Xigun Yan, Qin Cui, Bin Xu, Huiying Xu, Zhiping Cai *

Department of Electronic Engineering, Xiamen University, Xiamen 361005, China

ARTICLE INFO

Article history:
Received 12 March 2016
Received in revised form
8 June 2016
Accepted 9 June 2016
Available online 21 June 2016

Keywords:
Blue diode pump source
Pr:YLF visible lasers
Power scaling

ABSTRACT

We report a power scaled laser operation of diode-pumped Pr^{3+}-doped $LiYF_4$ crystal in single-end pumping geometry. Using a multi-mode InGaN diode laser, laser emissions at about 523.0, 604.1, 606.9, 639.4, 697.8 and 720.9 nm are achieved with maximum output power of 1.7, 0.6, 1.1, 2.3, 1.3 and 1 W, respectively. The corresponding slope efficiencies are found to be about 49%, 33%, 40%, 57%, 36% and 42%. Good laser beam qualities of these visible lasers are also found with measured beam propagation factors $M^2 < 1.8$ for all of them.

1. Introduction

High-power laser emissions in visible region have a wide range of applications not only in the entertainment industry, but also in the domain of scientific investigations, including large scale laser systems such as giant screen laser displays [1] and serving as laser pump sources with high photon energies for laser generation in mid-infrared spectral domain [2,3]. In industry, visible high-power lasers could process metals such as copper and gold which have a high reflectivity in the infrared spectral range precisely and efficiently [4]. What's more, visible high-power lasers could open access to UV or even Deep UV generation by frequency doubling with the aid of nonlinear crystals [5].

Pr^{3+}-doped materials could offer rich laser transitions in the blue, green, orange, red, and deep red spectral regions. Fluoride hosts, particularly YLF ($LiYF_4$), compared with the oxide hosts, have lower non-radiative multi-phonon decay and lower excited state absorption from the upper laser levels [6], interests have grown for Pr^{3+}-doped YLF to generate lasers in the visible spectral region. In order to achieve these visible lasers, the photons need to be pumped from ground-state level $^3H_4$ to excited energy level $^3P_0$ (around 480 nm), $^3P_1+^1I_6$ (around 469 nm), or $^3P_2$ (around 444 nm). Therefore, three efficient pump sources have ever been developed to meet the pumping demands, i.e., optically pumped and frequency-doubled semiconductor lasers (OPSLs) at ~480 nm [7], diode-pumped and frequency-doubled Nd:YAG laser at ~469 nm [8,9], and InGaN laser diodes at ~444 nm [10–12].

Power scaling to watt level of these Pr:YLF-based visible lasers has ever been reported using an OPSL in 2014, in which, e.g. a maximum output power up to 2.9 W in green was achieved [7]. However, at present, the OPSLs operating at the blue spectral domain are still expensive, cumbersome and on-demand. In contrast to OPSL blue laser sources, InGaN-based diode lasers provide advantages, such as compactness, low cost and commercial availability. In fact, in 2011, really efficient diode-double-end-pumped continuous-wave (cw) visible laser oscillations based on Pr:YLF have been demonstrated [13]. Pumped by two blue diode lasers of a Pr:YLF crystal, the authors demonstrated laser operation at 522.6, 545.9, 607.2 and 639.5 nm with maximum output powers of 773, 384, 418 and 938 mW, as well as slop efficiencies of 61.5%, 52.1%, 32% and 63.6%, respectively. However, up to now, InGaN laser diodes pumped Pr:YLF lasers have not reached watt level, as far as we know, including the high-gain red 639-nm laser emission.

In this paper, thanks to the recent availability of high-power blue diode laser, we report on the power scaling of visible Pr:YLF lasers at 523.0, 604.1, 606.9, 639.4, 697.8 and 720.9 nm, using a simple and compact diode-single-end-pumped geometry. For 523, 607, 639, 698 and 721 nm lasers, the maximum output powers were respectively improved to watt levels, for the first time to our knowledge.

2. Experimental details

The laser configuration used in the experiments is depicted in Fig. 1. The pump source is a commercially available InGaN blue LD. The LD itself was integrated with four individual laser diodes, with

* Corresponding author.
E-mail address: zpcai@xmu.edu.cn (Z. Cai).

http://dx.doi.org/10.1016/j.optcom.2016.06.026
0030-4018/

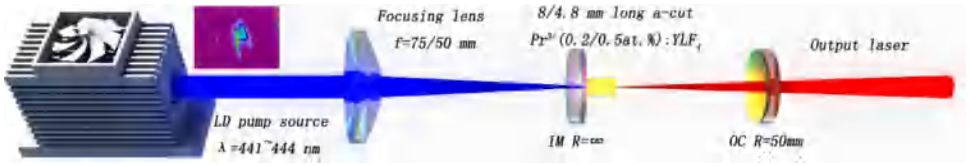

Fig. 1. The schematically experimental setup of diode-pumped Pr:YLF lasers.

which an aspheric lens (focal length $f=3$ mm) and a pair of cylindrical lenses ($f=-8$ and 40 mm) were used to collimate and to correct the astigmatism of the pump beam. The beam quality factor M^2 of the LD in x and y dimensions were measured to be 25.7 and 12.3, respectively. The beam quality depicted in Fig. 1 shows a clear multimode with two split stripes. The emitting peak wavelength of the pumping LD varies from 441 nm to 444 nm as the drive current changes from about 0.15 A (threshold) to maximum of 1.58 A, with a linewidth of about 1.7 nm (FWHM) at full power.

The laser resonator was a typical two-mirror linear cavity configuration. The coatings of the input mirror (IM) and output coupler (OC) used in our experiments were designed and fabricated in our lab by using plasma direct-current sputtering technology. All these flat dichroic IMs have high transmission $>91\%$ at pump wavelength and highly reflective coating at these considered visible laser wavelengths. For OCs (all with radii of curvatures of 50 mm), different mirrors with appropriate transmissions for these desired laser wavelengths were applied. The detailed descriptions of coatings with respect to these IMs and OCs will be introduced specifically in section three.

Three important factors have been considered during the design of the visible laser system. First of all, doping concentrations of the used Pr:YLF crystals were paid special cares. For laser operation at about 523, 640, 698 and 721 nm, since no reabsorption problem, a 0.5 at%-doped Pr:YLF crystal was used with length of 4.8 mm. In this condition, the laser crystal absorbed about 52% of the maximum pump power. The moderate concentration of the crystal was believed to be helpful in decreasing the probability of non-radiative cross-relaxation processes [13]. For orange laser operation at about 604 and 607 nm, we used a 8-mm-long Pr:YLF crystal with doing concentration of only 0.2 at%. The weakly doped laser crystal was proved to be favorable for the orange laser operation because of the reduced reabsorption loss [14,15]. The relatively long crystal as a compensation of the weak concentration improved the absorption ratio to about 48%. Moreover, the gain medium was nicely polished with uncoated plane parallel end faces. The crystal was placed very close to the IM, which was wrapped with indium foil and then mounted inside a copper block that was water cooled by a chiller (Huber Corp.) to control the temperature at 18°.

Secondly, special cares were also paid to the utilization of focusing lenses in order to extract the pump power as much as possible. For the 8-mm-long crystal, a 75-mm (focal length) positive lens was used to focus the pump beam into the laser crystal. However, for the 4.8-mm-long crystal, a 50-mm lens was used instead. Thirdly, instead of commonly used hemispherical laser cavity (i.e. with cavity length of about 50 mm), during the laser experiments, we configured the laser cavities to physical lengths of about 31–47 mm accordingly.

By using focusing lenses with different focal lengths to match the lengths of the laser crystals as well as adopting optimized cavity lengths, relatively good overlap efficiency between the pump beam and laser modes for all these visible lasers can be found. In fact, for a typical two-mirror plano-concave cavity, the laser cavity mode waist ω_0 can be determined by [16]

$$\omega_0 = \sqrt{\frac{L\lambda}{n\pi}}\left[\frac{g_1 g_2(1-g_1 g_2)}{(g_1+g_2-2g_1 g_2)^2}\right]^{1/4} \quad (1)$$

where L is the cavity length, λ is the wavelength of the emitting laser, n is the refractive index of the medium filling the resonator, $g_i \equiv 1 - L/R_i$ is the "g-factor" of the resonator and R_i ($i=1$ and 2) is the radii of curvature of the two mirrors. Then the overlap efficiency η_m could be resolved by $\eta_m = \omega_0/\omega_p$, where ω_p is the pump cavity mode waist which is measured to be 48 μm and 82 μm focused by 50-mm and 75-mm focus lens, respectively, by utilizing standard laser beam diagnostic equipment Spiricon M^2-200 (Spiricon M^2-200). In our experiments, the actual cavity lengths corresponding to the best performances of each laser emission are recorded in Table 1.

3. Results and discussion

Continuous-wave laser experiments with all these OCs were carried out at emission wavelengths of 523.0, 604.1, 606.9, 639.4, 697.8 and 720.9 nm. First of all, these laser spectra are shown in Fig. 2, which were measured by an HR4000 wavelength meter with a resolution of about 0.25 nm for 523 nm and by Hewlett Packard 8560E Series Optical Spectrum Analyzer with a resolution of 0.08 nm for the other wavelengths.

For the 639 nm laser, laser experiments using OCs with transmissions of 0.4%, 0.9%, 1.3%, 1.9%, 2.2%, 2.6%, 3.2%, 3.6% and 7.8% at the 639 nm were carried out. The best laser performance was achieved with maximum output power of 2.3 W and slope efficiency of 57% by using the 3.6% transmissive OC. In this specific case, since the 639 nm emission line possesses the highest emission cross section, it is not necessary to pay special care to suppression of other visible emissions, especially for the transmissions of the used OCs in this experiment were all not high. For

Table 1
Laser Parameters of the LD-Pumped Pr^{3+}:$LiYF_4$ Lasers.

λ_{em}(nm)	σ_{em}(10^{-20} cm^2)	T_{oc}(%)	P_{thr}(mW)	P_{max}(W)	L(mm)	η_m(%)	η_{sl}(%)	$2\gamma_{int}$(%)	M^2 at P_{max}
523	2.6	3.2	381	1.7	46	83	49	1.4	< 1.6
604	9.8	12.1	1145	0.6	35	80	33	9.4	< 1.7
607	13.6	7.6	784	1.1	31	83	40	3.9	< 1.5
639	21.8	3.6	51	2.3	47	83	57	0.1	< 1.5
698	5.2	0.9	78	1.3	47	84	36	0.4	< 1.6
721	8.8	2.2	100	1	47	82	42	0.4	< 1.8

Note: The respective laser curves can be found in Fig. 3.

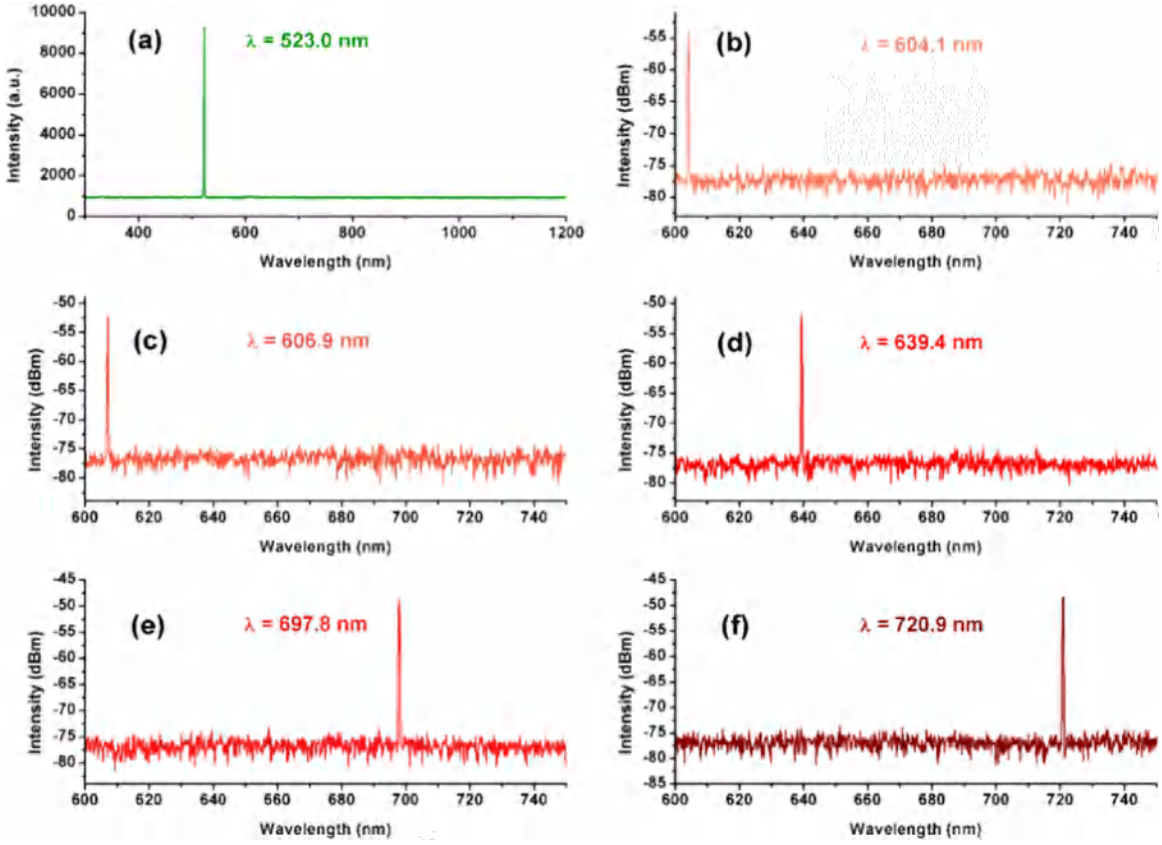

Fig. 2. Laser emissions at 523.0, 604.1, 606.9, 639.4, 697.8 and 720.9 nm.

instance, for the 3.6% transmissive OC, the transmissions are 68% at green, 7.2% at 604 nm, 6.5% at 607 nm, 5.2% at 698 nm and 8.6% at 721 nm.

Note that the 639 nm laser produced the highest output power and slop efficiency among all these visible laser emissions in our experiments. Since the output powers exhibited good linearity and no saturation can be observed, power scaling the 639 nm red laser to higher level could still be expected by employing a pump source with higher power. In addition, since the Pr:YLF crystal was only 4.8 mm leading to a weak absorption of the pump power, using a longer crystal to absorb much pump power should be favorable for improving the output power.

For the 523 nm laser experiments, the IM had a high reflection of $R > 99.9\%$ at 523 nm, and a transmission $T > 60\%$ around 607 and 639 nm to suppress the high gain emissions at those wavelengths. With the help of OCs with transmissions of 0.2%, 0.7%, 1.3%, 1.9%, 2.4%, 2.8%, 3.2% and 4.5% at 523 nm, laser emission at this wavelength was achieved. A relatively high slop efficiency of 49% and output power of 1.7 W was obtained with 3.2% transmissive OC for the green laser at 523 nm. The relatively high slope efficiency of the green laser, next to the highest red laser among all the visible lasers, can be explained as follows. Slope efficiency can be expressed as $\eta_{sl} = \eta_{Stokes}\eta_p\left[T_{OC}/(T_{OC} + 2\gamma_{int})\right]$, where $\eta_{Stokes} = \lambda_p/\lambda_l$ is the Stokes efficiency, η_p is the fraction of excited ions per absorbed pump photons (assumed to be unity), T_{OC} is the output mirror transmission and $2\gamma_{int}$ is the internal round-trip cavity losses. From this formula, one can see that green laser possesses the highest Stokes efficiency and therefore lowest heat generation. Moreover, the 523 nm laser generated from the so-called thermal coupled ^3P_J and $^1I_6$ multiplets and therefore an enlarged effective emission lifetime arising from the thermalization of the $^3P_1$, $^1I_6$ and $^3P_0$ levels was in general attained. The large effective emission lifetime could lead to increased effective emission cross section for the green laser transition [17].

For orange laser emissions, experiments were carried out with output mirror transmissions of 0.3%, 0.9%, 1.4%, 2.6%, 3.3%, 4.9%, 5.2%, 6.5% and 7.6% at 607 nm and 9.8%, 12.1% and 13.5% at 604 nm. To suppress the high-gain 639 nm emission, the used one IM had a transmission of 53% at 639 nm. Moreover, all the OCs had transmissions of more than 30% at 639 nm for further ensuring that the 639-nm line cannot lase. Maximum output powers of 1.1 W and 0.6 W were obtained with slope efficiencies of 40% and 33% at 607 and 604 nm with respect to the absorbed pump power, the corresponding transmission of OC was 7.6% at 607 nm and 12.1% at 604 nm and absorbed threshold pump power was 784 and 1145 mW, respectively. Experiments showed that orange lasers at 604 and 607 nm operated best at relatively high transmission of OC to overcome internal round-trip cavity losses originating in ground-state absorption into the $^1D_2$ level. Since the ground-state re-absorption for 604 nm transition is stronger than the 607 nm transition, it lased at a higher transmission of OC than the latter.

Deep red laser experiments at 698 nm and 721 nm were carried out with output mirror transmissions of 0.5%, 0.9% and 2.1% at 698 nm and 0.3%, 1.5%, 2.2%, 2.7% and 3.1% at 721 nm, respectively. Thanks to the IM with a high transmission of $> 36\%$ and to the OCs with transmissions of greater than 60% at the red and orange spectrum regions, the high gain emissions of 639, 607 and 604 nm were suppressed. With the 0.9% at 698 nm and 2.2% at 721 nm OC, the ones that achieved the best performance at the corresponding wavelength, maximum output powers of about 1.3 W and 1 W were extracted at 698 nm and 721 nm, leading to laser slope efficiencies of 36% and 42% with respect to the absorbed pump power, respectively.

The laser characteristics for the transmissions of OCs providing the highest output powers are depicted in Fig. 3.

As shown in Fig. 3, the lasers at 523 nm and 639 nm did not

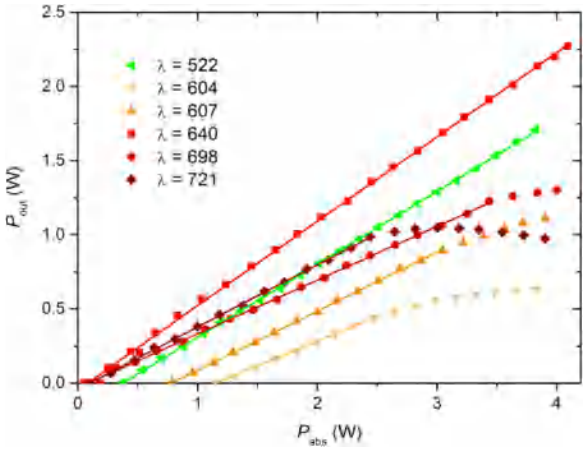

Fig. 3. The output power characteristics of the laser emissions at 523, 604, 607, 639, 698 and 721 nm. The respective transmissions of OCs can be found in Table 1.

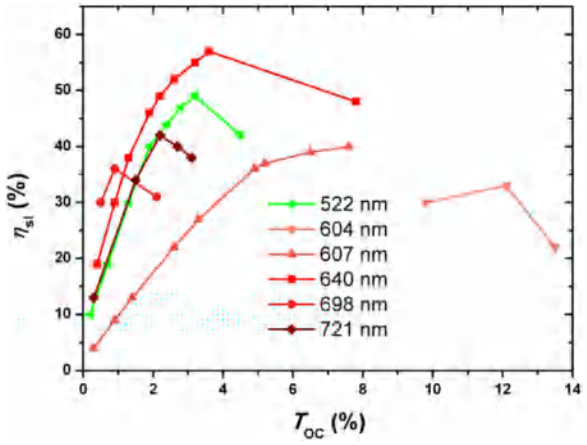

Fig. 4. Dependency of the slope efficiency on the output coupling transmission for continuous-wave Pr^{3+}:$LiYF_4$ lasers operated at different wavelengths.

show any thermal rollover even for the highest pump power. However, laser emissions in the deep red spectrum region exhibited thermal saturation to some extent, which might be caused by larger quantum defect. For orange lasers, the output power might be restricted to great extent by the ground-state reabsorption.

The corresponding η_m is calculated to be 80∼84%, which shows a good agreement with our assumption.

For all lasers except the orange, we estimated the internal round-trip cavity losses $2\gamma_{\text{int}}$: in the light of the energy conservation law, the internal round-trip cavity losses for the corresponding transmission of OC could be determined in [7].

$$2\gamma_{\text{int}} \leq -\ln(1-T_{OC})\cdot\left(\frac{\eta_{Stokes}}{\eta_{sl}}-1\right) \tag{2}$$

For the output mirror transmissions of 3.2%, 12.1%, 7.6%, 3.6%, 0.9%, 2.2% at wavelengths of 523, 604, 607, 639, 698 and 721 nm, the internal round-trip cavity losses is calculated to be 1.4%, 9.4%, 3.9%, 0.1%, 0.4% and 0.4%, respectively. For the orange lasers the estimations do not result in reasonable values because of the $^3H_4 \rightarrow {}^1D_2$ re-absorption at the laser wavelengths.

The variations of slop efficiencies versus transmissions of OCs for the different wavelengths are depicted in Fig. 4. As is shown, firstly, with the increasing of the transmissions of the OCs, the slope efficiencies increased accordingly. However, secondly, when the slope efficiencies reached the maximum values (corresponding to optimized transmissions of the OCs), it decreased when further increasing the transmissions of the OCs. Apart from the orange ones, all lasers exhibit maximum slope efficiencies at relatively low transmissions of OCs between 1% and 5% and slop efficiencies drop significantly at higher transmissions of OCs. For the orange lasers, the slope efficiency reached maximum at a higher transmissions of OCs.

In the end, the beam quality factors M^2, which were measured by using Spiricon M^2-200, were determined to be < 1.8 for the six lasers with the highest output power at maximum pump power. A summary of the parameters of the characterized lasers is given in Table 1.

4. Conclusion

In this paper, we presented the power scaling of diode-single-end-pumped visible Pr:YLF lasers at wavelengths of 523.0, 604.1, 606.9, 639.4, 697.8 and 720.9 nm. At these wavelengths, we obtained maximum output powers of 1.7, 0.6, 1.1, 2.3, 1.3 and 1 W and slop efficiencies of 49%, 33%, 40%, 57%, 36% and 42%, respectively, by implementing these laser experiments using compact two-mirror plano-concave laser cavities. As far as we know, this is heretofore the first demonstration of diode-pumped watt-level Pr:YLF lasers at 523, 607, 639, 698 and 721 nm. We expect that the output powers of all these visible laser emissions can be further scaled to higher levels in the near future by employing a pump source with better beam quality and by optimizing the laser gain medium.

Acknowledgments

The authors wish to acknowledge the financial support from the National Natural Science Foundation of China (61275050 and 61575164), the Specialized Research Fund for the Doctoral Program of Higher Education (20120121110034 and 20130121120043), the Fundamental Research Funds for the Central Universities (2013121022) and Natural Science Foundation of Fujian Province of China (2014J01251).

References

[1] O. Halabi, N. Chiba, Displays 30 (2009) 97.
[2] X. Zhang, J.P. Jouart, G. Mary, X. Liu, J. Yuan, J. Lumin. 983 (1997) 72–74.
[3] J.A. Creighton, D.G. Eadon, J. Chem. Soc. Faraday Trans. 87 (1991) 3881.
[4] S. Engler, R. Ramsayer, R. Poprawe, Phys. Procedia 12 (2011) 339.
[5] Z. Liu, Z.P. Cai, B. Xu, C.H. Zeng, S.L. Huang, F.J. Wang, Y. Yan, H.Y. Xu, IEEE Photonics J. PJ-5 (2013) 1500905.
[6] Z. Liu, Z.P. Cai, S.L. Huang, C.H. Zeng, Z.Y. Meng, Y.K. Bu, Z.Q. Luo, B. Xu, H.Y. Xu, C.C. Ye, F. Stareki, P. Camy, R. Moncorgé, J. Opt. Soc. Am. B 30 (2013) 302.
[7] P.W. Metz, F. Reichert, F. Moglia, S. Müller, D.T. Marzahl, C. Kränkel, G. Huber, Opt. Lett. 39 (2014) 3193.
[8] B. Xu, P. Camy, J.L. Doualan, A. Braud, Z. Cai, F. Balembois, R. Moncorgé, J. Opt. Soc. Am. B 29 (2012) 346.
[9] B. Xu, P. Camy, J.L. Doualan, Z. Cai, R. Moncorgé, Opt. Express 19 (2011) 1191.
[10] A. Richter, E. Heumann, E. Osiac, G. Huber, W. Seelert, A. Diening, Opt. Lett. 29 (2004) 2638.
[11] A. Richter, E. Heumann, G. Huber, V. Ostroumov, W. Seelert, Opt. Express 15 (2007) 5172.
[12] K. Hashimoto, F. Kannari, Opt. Lett. 32 (2007) 2493.
[13] T. Gün, P. Metz, G. Huber, Opt. Lett. 36 (2011) 1002.
[14] B. Xu, Z. Liu, H. Xu, Z. Cai, C. Zeng, S. Huang, Y. Yan, F. Wang, P. Camy, J. L. Doualan, A. Braud, R. Moncorgé, Opt. Commun. 305 (2013) 96–99.
[15] Yongjie Cheng, Bin Xu, Biao Qu, Saiyu Luo, Han Yang, Huiying Xu, Zhiping Cai, Appl. Opt. 33 (2014) 7898.
[16] A. Siegman, Lasers, University Science Boks, Mill Valley, 1986 (Chapters 19 and 11).
[17] S. Khiari, M. Velazquez, R. Moncorge, J.L. Doualan, P. Camy, A. Ferrier, M. Diaf, J. Alloy. Compd. 451 (2008) 128–131.